The Open Access Journal of Science and Technology
Vol. 2 (2014), Article ID 101048, 8 pages
doi:10.11131/2014/101048

AgiAl Publishing House
http://www.agialpress.com/

Research Article

Magnetic Resonance Imaging of the Normal Stifle Joint in Buffaloes (*Bos Bubalis*): an Anatomic Study

M. S. Sherif, M. Attia, H. Bahgaat, and A. Kassab

Department of Anatomy and Embryology, Faculty of Veterinary Medicine, Benha University, Egypt

Corresponding Author: A. Kassab; email: kassab_aa@yahoo.com

Received 29 November 2013; Accepted 3 August 2014

Academic Editor: Maria Elena Padin-Iruegas

Copyright © 2014 M. S. Sherif et al. This is an open access article distributed under the Creative Commons Attribution License, which permits unrestricted use, distribution, and reproduction in any medium, provided the original work is properly cited.

Abstract. The aim of the present study was to describe the normal anatomy of the stifle joint in buffaloes (*Bos bubalis*) on magnetic resonance images and related anatomical sectional slices to facilitate the interpretation of all these images, as well as to understand the basis for diseases diagnosis. The hind limbs of ten healthy adult buffaloes (Twenty stifle joints) were used. After slaughtering, MR images were made in sagittal, transverse, and dorsal planes. The limbs then were frozen at -20° then correspondingly sectioned using an electric band saw. Clinically relevant anatomic structures were identified and labeled at each level in the corresponding images (MR and anatomic slices). MRI images were used to identify the bony and soft tissue structures of the stifle joint. The articular cartilage appeared with hyperintense signal and separated from the subcondral bone by gray line (moderate signal intensity). It is difficult to differentiate between the synovia, infrapatellar fat body and the articular cartilage because they appeared with hyperintense signal. The meniscial, femoropatellar and cruciate ligaments recognized as moderate signal intensity. However, the collateral and intermediate patellar ligaments, the common tendon of the Mm. extensor digitorum longus and peroneus tertius as well as the menisci and the medial patellar fibrocartilage appeared with hypointense signal. The knowledge of normal anatomy of the buffalo stifle joint would serve as initial reference to the evaluation of MR images in this species.

Keywords: Author please provide

1. Introduction

Magnetic resonance Imaging (MRI) is widely used in the diagnosis of human musculoskeletal disease [30]. Superior soft tissue image resolution along with the ability to image in multiple planes has made MR imaging the diagnostic modality of choice for numerous joint conditions.

Diseases of the stifle joint in the ruminants are common, especially in the buffalo, which necessitates awareness of its normal structure to be able to recognize changes in the diseased animal. The stifle joint is often subject to surgical problems as patellar luxation, gonitis (stifle arthritis), synovitis, fracture, meniscial tearing and cruciate ligament sprain in the bovine [32].

Economic importance of the bovine lameness is completely understood, and many researches have been done in this filed for better understanding of the pathogenesis of the bovine stifle problems [27].

The bovine stifle is a complex structure with joints, ligaments and tendons [18]. Classical anatomic atlases can't provide the spectrum of views and the required details in modern diagnostic and surgical techniques [12].

Current diagnostic imaging technique such as radiography and ultrasonography provides limited information for evaluation of the bovine digits and hoof. Magnetic resonance imaging (MRI) gives more additional information on soft tissue and osseous injuries [9, 11]. Tendons and ligaments are more distinguishable with MRI if it's compared to computed tomography or ultrasonography [4, 20]

To our knowledge, a detailed comparative study of normal gross and MRI sections of the buffalo stifle has not been conducted. So, the aim of the present study is to describe the normal anatomy of the stifle joint in buffaloes (*Bos bubalis*) on magnetic resonance images and correlate anatomical cross-sectional slices with the obtained images to facilitate the interpretation of all these images.

2. Materials and Methods

Animals-The present work was carried out on twenty stifle joints of ten healthy buffaloes, 7 males and 3 females. The age ranged from 10–17 months. The selected animals were subjected to clinical, radiographic and ultrasonographic examinations before slaughtering; no abnormalities were detected. Three hind limbs were collected from freshly slaughtered animals in the teaching farm at the Faculty of Veterinary Medicine and the Faculty of Agriculture, Benha University, Egypt and other seven hind limbs were obtained from Benha slaughterhouse. Immediately after slaughtering, limbs were cooled and imaged within 12 hours to minimize post-mortem changes.

MRI examination-The limbs were consecutively undergone Magnetic Resonance Imaging using SIGNA HDe 1.5 TGE MRI scanner; by placing in a torso phased array coil (2 Tesla) for the sagittal and dorsal scans and in a body coil (2 Tesla) for the transverse scans, 5 mm slicing as indicated by [31] in equine MRI. Scanning details (as TR, TE and others) found in the MR images. Then, MR images of the comparable stifles were reformatted with a software E-film.

After the MR images were obtained, the limbs articular capsule were distended by either red or bleu colored gum milk latex [7]

Immediately after injection, the joints were flexed and extended 100 times and frozen at -20˚. The limbs then were sectioned using an electric band saw, as corresponding MR images. All sections were cleaned, photographed and kept for the future studies.

Comparison of MR and anatomic images-Important anatomic structures were recognized and labeled in two related MR scans and gross-sections of the buffalo stifle joint with the aid of multiple references [13, 23, 26], together with [24]. Ten photos from both MRI and gross sections were chosen for publication. Some structures present in the anatomical sections could not be seen on the corresponding MR images and vice versa.

3. Results

From the collection of matched MR and anatomic images, 3 representative sagittal combinations were selected (Figures 1-3), 4 cross sections (Figures 4–7), and 3 dorsal combinations (Figures 8–10). On each MR image, a further two small photos were put to clarify the section level. On the anatomic slices, it was possible to identify all muscles, tendons, and ligaments surrounding the stifle joint.

The bone surfaces could be easily identified in all MR images. The compact bone appeared with hypointense signal while spongy bone showed heterogenous signal intensity due to high fat content in the bone marrow and trabecular pattern. There was a regular and obviously distinct corticocancellous junction, as well. The distal epiphysis of the femur and proximal diaphysis of the tibia ossification centers appeared as irregular line of homogenous hypointense signal. The articular cartilage appeared as hyperintense structure and separated from the bone by gray line (moderate signal intensity) that represented the subcondral bone. The signal intensity of the articular cartilage was somewhat as the same as synovia.

The intermediate, medial and lateral patellar ligaments were recognized as hypointense signal structures and converge distally. The medial and lateral femoropatellar ligaments, the cranial and caudal meniscotibial ligaments and the meniscofemoral ligament of lateral meniscus appeared with moderate signal intensity (Figures 1, 3, and 10). The cranial and caudal cruciate ligaments were recognized as moderate signal intensity bands (Figure 7). The cranial cruciate ligament consisted of two strata; craniomedial and caudolateral. Both strata extended proximally from the medial wall of the lateral femoral condyle; The craniomedial stratum inserted in lateral wall of the medial intercondyloid tubercle in the central intercondyloid fossa while The caudolateral stratum ended in the central intercondyloid fossa (Figure 6). The Caudal cruciate ligament passed medially to the cranial cruciate ligament. It extended proximally from the femoral intercondylar fossa and inserted in the popliteal notch (Figure 7). The medial patellar fibrocartilage (Figures 2 and 3) appeared with hypointense signal and acted as origin for the medial patellar ligament and as insertion of the medial femoropatellar ligament.

The common tendon of Mm. extensor digitorum longus and peroneus tertius (Figure 9) recognized as hypointense signal structures as well. The infrapatellar fat body interposed between the synovial and fibrous layers of the articular capsule and occupy the space which is formed by the patella proximally, the tibial condyles distally, the femoral condyle caudally and the patellar ligaments cranially. It separated the patellar ligament from the meniscus caudally and appeared as hyperintense signal structure so it is difficult to differentiate from the synovia because both are with the same intensity (Figure 3).

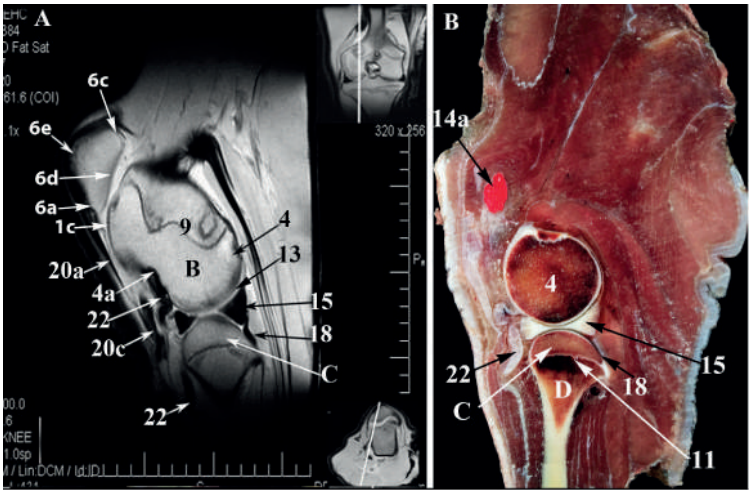

Figure 1: Sagittal MR image (A) and gross anatomic section (B) of the left buffalo stifle at the level of 3 cm lateral to the Fossa intercondylaris (dorsal is up and caudal is to the right of the viewer). A, Corpus ossis femoris ; B, Distal epiphysis of os femoris; C, Extremitas proximalis tibiae; D, Corpus tibiae; 1, Trochlea ossis femoris (1a, medial ridge; 1c, intertrochlear groove); 2, Facies popliteal; 3, Condylus medialis of os femoris; 4, Condylus lateralis of os femrois (4a, Fossa extensoria); 6, Patella (6a, Basis patellae; 6b, Processus cartilaginous; 6c, Apex patellae; 6d, Facies articularis; 6e, Facies cranialis); 7, Condylus lateralis of the tibia (7a, Incisura Poplitea); 8, Tuberositas tibiae; 9, Distal epiphysis of the femur ossification center; 10, Tibial tuberosity ossification center; 11, Proximal diaphysis of the tibia ossification center; 12, medial femorotibial sac; 13, lateral femorotibial sac; 14, femoropatellar synovial sac (14a, proximal pouch); 15, Meniscus lateralis (15a, cranial meniscotibial ligament; 15b, Lig. Meniscofemorale); 16, Meniscus medialis (16a, cranial meniscotibial ligament); 17, Ligg. Cruciata genus (17a, Lig. cruciatum craniale; 17b, Lig. cruciatum caudale); 18, Lig. popliteum obliquum; 19, Fibrocartilagines parapatellaris medialis; 20a, Lig. patellae intermedium; 20b, Lig. patellae mediale; 20c, Lig. patellae laterale; 21, Corpus adiposum infrapatellare; 22, Common tendon of the extensor digitorum longus and peronaeus tertius; VM, M. vastus medialis; VI, M. vastus intermedius; GL, M. gastrocnemius (Caput laterale);GM, M. gastrocnemius (Caput mediale); SD, M. flexor digitorum superficialis; POP, M. popliteus; ST, M. semitendinosus; SM, M. semimembranosus.

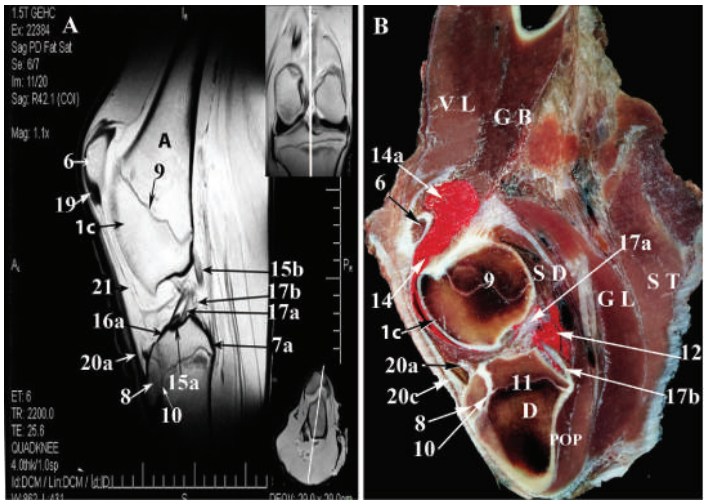

Figure 2: Sagittal MR image (A) and anatomic section (B) of the left buffalo stifle at the middle of the Fossa intercondylaris (dorsal is up and caudal is to the right of the viewer). Abbreviations as previous.

The Menisci showed homogenous very hypointense signal in MRI and present between the femoral and tibial condyles articular cartilages to divide the medial and lateral Femorotibial joint cavities partially into two compartments for each; The Proximal sac formed between the proximal surface of the meniscus and the femoral condyle articular cartilage while the distal sac formed between the distal surface of the meniscus and the tibial condyle articular cartilage (Figures 1 and 10). Both proximal and distal Lateral femorotibial compartments (Figure 10) were continuous medially at the area between the lateral femoral and tibial condyles, where they were directly contacted. The proximal and distal medial femorotibial compartments (Figure 3) were continuous at the axial notched border of the medial meniscus

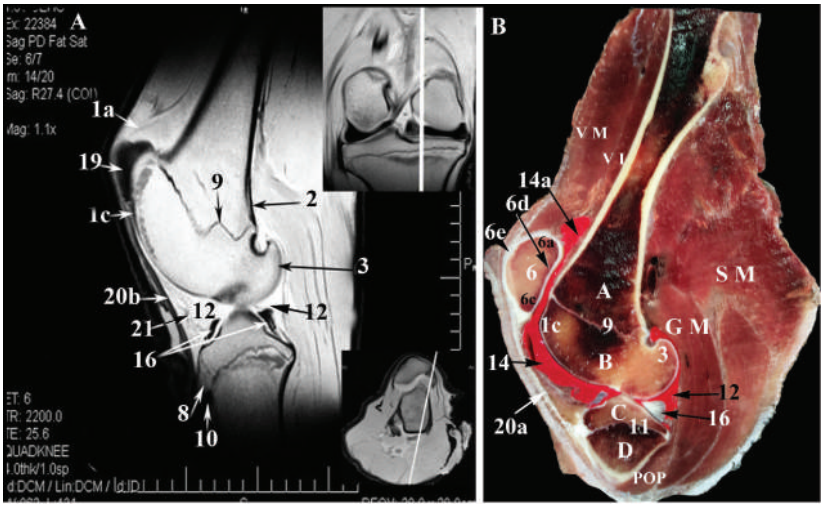

Figure 3: Sagittal MR image (A) and gross anatomic section (B) of the right buffalo stifle at 1cm medial to the fossa intercondylaris at the most lateral part of the Condylus medialis of the Os femoris (dorsal is up and caudal is to the right of the viewer). Abbreviations as previous.

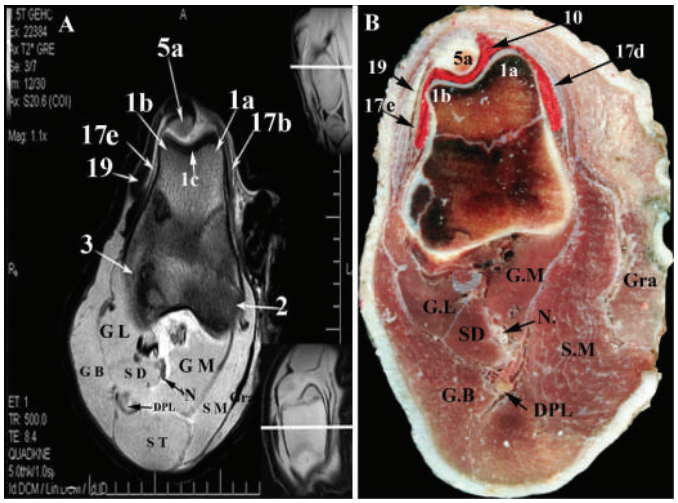

Figure 4: Transverse MR image (A) and gross anatomic section (B) of the left buffalo stifle at the level of the patellar apex (dorsal is up and lateral is to the left of the viewer). 1, Trochlea ossis femoris (1a, medial ridge; 1b, lateral ridge; 1c, intertrochlear groove); 2, Condylus medialis of os femoris; 3, Condylus lateralis of os femoris; 3a, Fossa extensoria; 4, Fossa intercondylaris; 5a, Apex patellae; 6, Eminentia intercondylaris (6a, tuberculum intercondylare mediale; 6b, tuberculum intercondylare laterale); 9, medial femorotibial synovial sac; 10, femoropatellar synovial sac; 11, Meniscus Lateralis; 11a, cranial meniscotibial ligament of the lateral meniscus; 11b, Lig. Meniscofemorale of the lateral meniscus; 12, Meniscus medialis; 12a, cranial meniscotibial ligament; 12b, caudal meniscotibial ligament; 13a, Lig. cruciatum craniale; 13b, Lig. cruciatum caudale; 14, Lig. collaterale laterlae; 15, Lig. collaterale mediale; 16, Lig. popliteum obliquum; 17a, Lig. patellae intermedium; 17b, , Lig. patellae mediale; 17c, Lig. patellae laterale; 17d, Lig. femoropatellare mediale; 17e, Lig. femoropatellare laterale; 18, Corpus adiposum infrapatellare; 19, Gluteobiceps tendon; 20, Common tendon of the extensor digitorum longus and peronaeus tertius; T, proximal Extremity of the tibia; DPL, Deep popliteal lymph node; GL, M. gastrocnemius (Caput laterale); GM, M. gastrocnemius (Caput mediale); SD, M. flexor digitorum superficialis; POP, M. popliteus; GB, M. gluteobiceps femoris; ST, M. semitendinosus; SM, M. semimembranosus; Gra, M. gracilis.

at the area between the medial femoral and tibial condyles. The proximal compartment of the medial femorotibial sac was continuous freely at level of the ridge connecting between the medial trochlear ridge and medial femoral condyle with the femoropatellar synovial sac but at the same time, it was separated from lateral femorotibial synovial sac at the level of the cruciate ligament decussating above the central tibial intercondylar fossa. The lateral meniscus didn't cover the caudolateral part of the lateral tibial condyle because this part was covered by the tendon of origin of the M. popliteus to separate the lateral meniscus from the lateral collateral ligament of the femorotibial joint. The lateral meniscus was separated from the tendon of origin of the M. popliteus by lateral Femorotibial synovial pouch that act as a

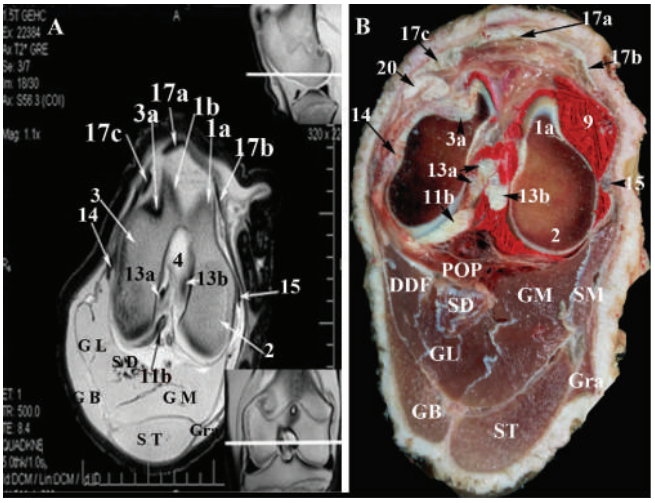

Figure 5: Transverse MR image (A) and gross anatomic section (B) of the left buffalo stifle at the level of the proximal parts of the Eminentia intercondylaris (dorsal is up and lateral is to the left of the viewer). Abbreviations as previous.

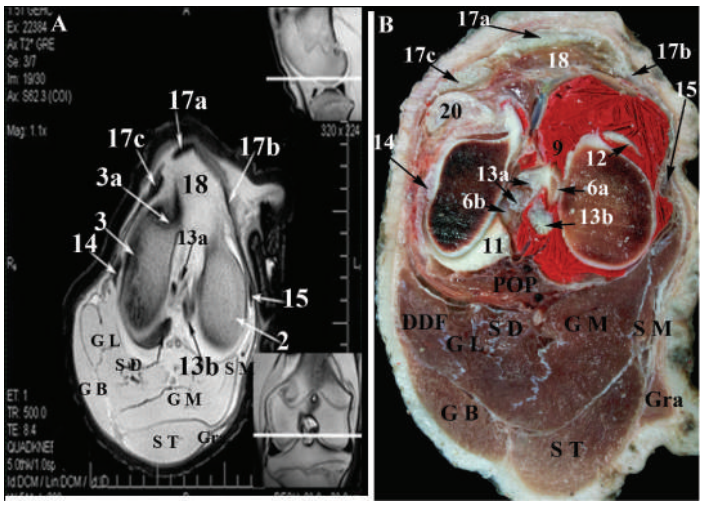

Figure 6: Transverse MR image (A) and gross anatomic section (B) of the left buffalo stifle at the level the base of the Eminentia intercondylaris and most distal parts of the femoral condyles (dorsal is up and lateral is to the left of the viewer). Abbreviations as previous.

bursa (Figure 10). The tendon of origin of the M. popliteus appeared as a hypointense signal structure.

The proximal and distal femorotibial sacs appeared as a thin line of hyperintense signal proximal and distal to the lateral meniscus respectively (Figures 1, 6, and 10). The femoropatellar synovial sac appeared with hyperintense signal as well (Figure 3). It had a pouch proximally for about 6 cm to form suprapatellar pouch where it is separated from the overlying two portions of the M. vastus intermedius by fatty tissue.

4. Discussion

The present study serves as an initial reference that aid in MR imaging diagnosis of the buffalo stifle disorders. Knowledge of normal cross sectional anatomy of the buffalo stifle joint is essential for the evaluation of MRI scans. MR images of the buffalo stifle provide acceptable details of the anatomical structures with corresponding gross specimens.

Radiography has limited value to evaluation of soft tissue. Although ultrasonography provides visualization of the tendons and ligaments [17], it provides a small field of view and each structure has to be imaged separately. On the other hand, soft tissue is difficult to be evaluated by ultrasonography as a cross sectional examination through the entire digit is not possible [6].

MRI scan is excellent imaging modality, however, Its usage in veterinary medicine is limited as it is expensive and the animal should be anaesthetized [1]. Nevertheless, it has some potential advantages over the routine radiography; it provides a cross-sectional image with superior soft tissue

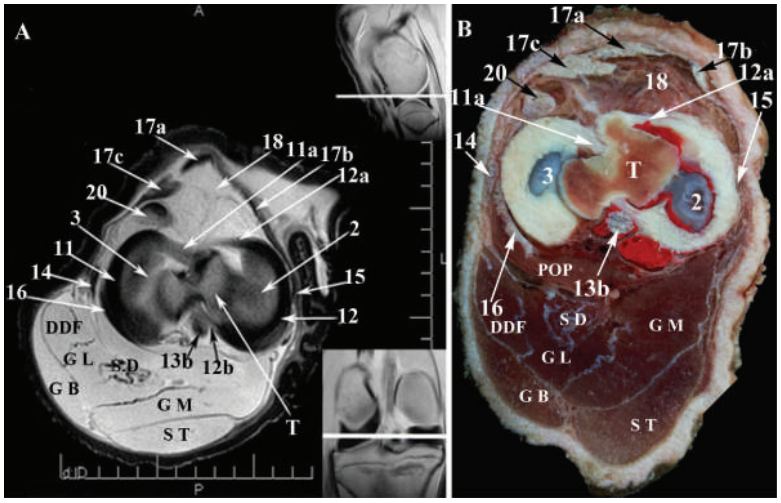

Figure 7: Transverse MR image (A) and gross anatomic section (B) of the left buffalo stifle at the level of the menisci (dorsal is up and lateral is to the left of the viewer). Abbreviations as previous.

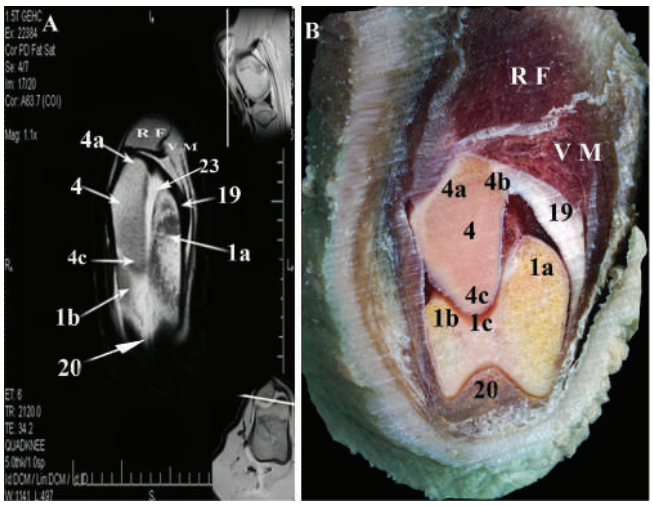

Figure 8: Dorsal MR image (A) and gross anatomic section (B) of the left buffalo stifle 2cm caudal to the most cranial part of trochleae ossis femoris (dorsal is up and lateral is to the left of the viewer). 1, Trochlea ossis femoris (1a, medial ridge; 1b, lateral ridge; 1c, intertrochlear groove); 2, Condylus medialis of os femoris; 3, Condylus lateralis of os femoris; 3a, Fossa extensoria; 4, patella; (4a, Basis patellae; 4b, Processus cartilagineus; 4c, Apex patellae); 5, Condylus medialis of the tibia; 6, Condylus lateralis of the tibia; 7, Eminentia intercondylaris; 7a, tuberculum intercondylare mediale; 7b, tuberculum intercondylare laterale; 8, Tuberositas tibiae; 10, Distal epiphysis of the femur ossification center; 11, Proximal diaphysis of the tibia ossification center; 12, lateral femorotibial sac (12a, distal pouch); 13, Meniscus lateralis; 14, Lig. Meniscofemorale; 15, Meniscus medialis; 15a, caudal meniscotibial ligament, 16a, Lig. cruciatum craniale; 16b, Lig. cruciatum caudale; 17, Lig. collaterale laterlae;18, Lig. popliteum obliquum; 19, Fibrocartilagines parapatellaris medialis; 20, Lig. patellae intermedium; 21, Common tendon of the extensor digitorum longus and peronaeus tertius; 22, Popliteal artery and vein; 23, Femoropatellar joint; VM, M. vastus medialis; RF, M. rectus femoris; GL, M. gastrocnemius (Caput laterale); GM, M. gastrocnemius (Caput mediale); SDF, M. flexor digitorum superficialis; GB, M. gluteobiceps femoris.

differentiation and no superimposition of the overlying structures, which can be used for better diagnosis of abnormalities [25].

The signal intensities in the cadaver specimens can be different in live animals because of the loss of fluid and blood in the cadavers, the freezing and absence of blood flow, however, the gross anatomy is the same [7, 31] in horses.

Our results reveal that the compact bone appears with hypointense signal while the spongy bone with moderate intensity. Such findings come in agreement with [14, 31] in horses.

The articular cartilage shows hyperintensity and separate from the bone by gray line (moderate signal intensity).These results agree with [29] in the dog and disagree with [14, 31]

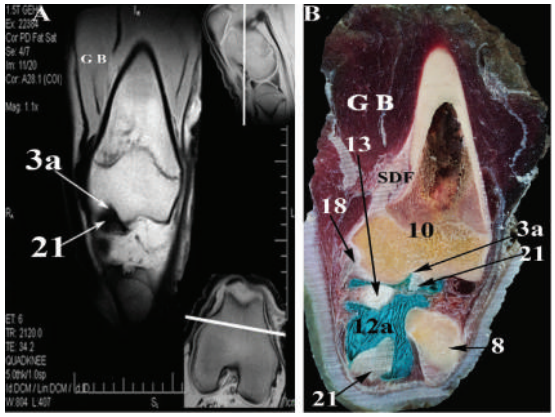

Figure 9: Dorsal MR image (A) and gross anatomic section (B) of the left buffalo stifle at the level of the Fossa extensoria (dorsal is up and lateral is to the left of the viewer). Abbreviations as previous.

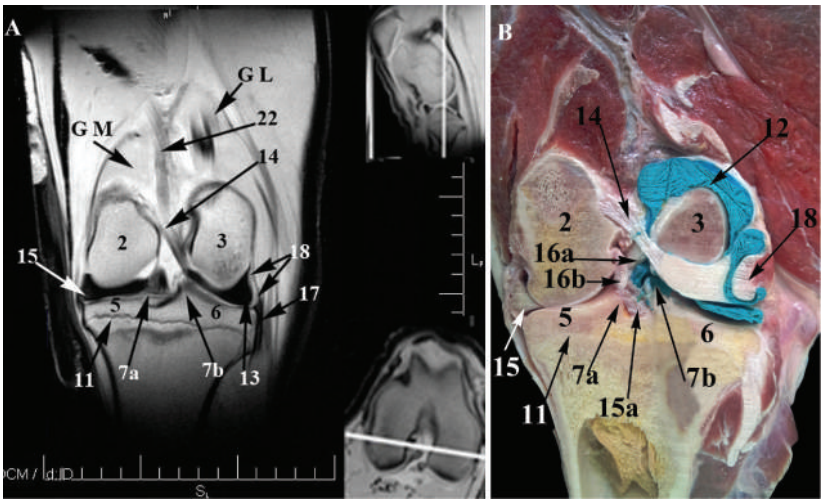

Figure 10: Dorsal MR image (A) and gross anatomic section (B) of the buffalo right stifle at the level of the Area intercondylaris centralis (dorsal is up and lateral is to the right of the viewer). Abbreviations as previous.

in the horse who recognized the articular cartilage as a layer of homogenous moderate signal intensity.

The medial and lateral menisci were imaged with hypointense signal as mentioned by [14, 16, 31] in the horse and [29] in the dog. However, [22] in the horse reported that the medial and lateral menisci ranged from moderate to low signal intensity depending on Tesla used.

The intermediate, medial and lateral patellar ligaments appeared with hypointense signal that comes parallel with the results of [14, 22, 31] in the horse; [29] in the dog and [11] in the dog and the cat.

The infrapatellar fat body appears as hyperintense signal so it was be difficult to differentiate with the synovial capsule because both appear with the same intensity which resemble to results by [14, 22] in the horse.

The medial and lateral femorotibial synovial sacs are separated at the level of the cruciate ligament decussation which agree with [8, 15] in the ruminants, [2, 5, 19, 28] in the horse and [21] in the dog and disagree with [10] in the goat who stated that both medial and lateral sacs are connected inferior to cruciate ligament decussation.

5. Conclusion and clinical relevance

The knowledge of normal anatomy of the buffalo stifle joint on MR images is necessary to provide an accurate interpretation of these images. This study is a preliminary step toward the clinical use of MR in soft tissue injuries of the stifle in the buffalo, but more investigations may be attempted to evaluate the effective advantage of MR in the diagnosis of these conditions.

Acknowledgment

The authors wish to thank Prof. Dr. Ahmed Faried, professor of human diagnostic imaging and Dr. Amr Raslan, Head of

Tanta Scan diagnostic imaging laboratory, for their valuable assistance in the practical part of this study.

References

[1] A. Arencibia, J. M. Vázquez, M. Rivero, R. Latorre, J. A. Sandoval, J. M. Vilar, and J. A. Ramírez, Computed tomography of normal cranioencephalic structures in two horses, *Anatomia, Histologia, Embryologia*, **29**, no. 5, 295–299, (2000).

[2] K. D. Budras, W. O. Sack, and S. Rock, Anatomy of the horse, in *Chapter 3: Pelvic Limb*, K. G. Hans-Böckler-Alle, Ed., Schlütersche Verlagsgesellschaft mbH & Co., Hannover, Germany, 5th edition, 2009.

[3] J. E. Carter, T. Saveraid, M. Rick, and D. Herthel, *Magnetic Resonance Imaging of the Equine Stifle in a Clinical Setting*, American College of Veterinary Surgeons Surgical Summit, Chicago, Ill, USA, 2007.

[4] C. R. Cook, MRI of the canine stifle joint, in *Proceedings of the 3rd World Veterinary Orthopaedic Congress, ESVOT-VOS 15th ESVOT Congress*, University of Missouri-Columbia, Bologna, Italy, September 2010.

[5] A. De Lahunta and R. E. Habel, *Applied Veterinary Anatomy*, Library of Congress Cataloging in Publication Data, W.B. Saunders, Philadelphia, Pa, USA, 1986.

[6] J. M. Denoix, N. Crevier, B. Roger, and J. F. Lebas, Magnetic resonance imaging of the equine foot, *Veterinary Radiology & Ultrasound*, **34**, no. 6, 405–411, (1993).

[7] K. M. Dyce, W. O. Sack, and C. J. G. Wensing, *Textbook of Veterinary Anatomy*, W. B. Saunders, Philadelphia, Pa, USA, 2nd edition, 1987.

[8] R. A. Elhanbaly, *Why the incidence of the upward fixation of the patella is higher in Buffalo than in Cattle? [M.S. thesis]*, Assiut University, 2011.

[9] J. H. Foreman, Use of magnetic resonance imaging in equine lameness diagnosis, *Pferdeheilkunde*, **12**, no. 4, 686–687, (1996).

[10] M. R. A. Gad, *Some anatomical studies on the genual articulation of the goat [M.S. thesis]*, Cairo University, 1979.

[11] P. R. Gavin and S. P. Holmes, Practical small animal MRI, in *Chapter 3: Orthopedic*, P. R. Gavin and R. S. Bagley, Eds., 233–273, Wiley-Blackwell Library of Congress Cataloging-in-Publication Data, 1st edition, 2009.

[12] S. Gehrmann, K. H. Höhne, W. Linhart, B. Pflesser, A. Pommert, M. Riemer, U. Tiede, J. Windolf, U. Schumacher, and J. M. Rueger, A novel interactive anatomic atlas of the hand, *Clinical Anatomy*, **19**, no. 3, 258–266, (2006).

[13] R. Getty, *The Anatomy of the Domestic Animals*, **1**, WB Saunders, Philadelphia, Pa, USA, 5th edition, 1975.

[14] S. J. Holocombe, A. L. Bertone, D. S. Biller, and V. Haider, Magnetic resonance imaging of the equine stifle, *Veterinary Radiology & Ultrasound*, **36**, 119–125, (1995).

[15] I. S. Ibrahim and M. S. Moustafa, Some anatomical observation on the stifle joint of the buffalo in Egypt, *Veterinary Medical Journal*, **23**, 123–132, (1977).

[16] C. E. Judy, Magnetic resonance imaging of the equine stifle, *Veterinary Radiology & Ultrasound*, **52**, 479–484, (2011).

[17] B. Kaser-Hotz, S. Sartoretti-Schefer, and R. Weiss, Computed tomography and magnetic resonance imaging of the normal equine carpus, *Veterinary Radiology & Ultrasound*, **35**, 457–461, (1994).

[18] A. Kassab and A. Badawy, Ultrasonographic anatomy of the patellar ligaments before and after medial patellar desmotomy in buffaloes (Bos bubalis), *Emirates Journal of Food and Agriculture*, **23**, no. 5, 460–465, (2011).

[19] H. E. Konig and H. G. Liebich, Veterinary anatomy of domestic mammals, in *Chapter 4; Pelvic Limb*, Text Book and Color Atlas, Schattauer GmbH, Holderlinestrabe, Stuttgart, Germany, 2004.

[20] T. S. Mair, J. Kinns, R. D. Jones, and N. M. Bolas, Magnetic resonance imaging of the distal limb of the standing horse, *Equine Veterinary Education*, **17**, no. 2, 74–78, (2005)., Technique and Review of 40 Cases of Foot Lameness Proceedings of the 49th Annual Convention of the American Association of Equine Practitioners, New Orleans, Lo, USA, 2003.

[21] M. E. Miller, G. C. Chrisetensen, and H. E. Evans, Anatomy of the dog, in *Chapter 2—Arthrology*, W.B Saunders, Philadelphia, Pa, USA, 1979.

[22] R. Murray, N. Werpy, F. Audigié, J. Denoix, M. Brokken, and T. Schulze, *Equine MRI of the Proximal Tarsal Region*, **421** of *Edited by R. C. Murray*, Blackwell Publishing, 2011.

[23] R. Nickel, A. Schummer, and E. Seiferle, *The Anatomy of Domestic Animals*, **2**, Blackwell Science, Oxford, UK, 1996.

[24] , *International Committee on Veterinary Gross Anatomical Nomenclature of the World Association of Veterinary Anatomists*, 5th edition, 2005.

[25] A. R. Raji, K. Sardari, and H. R. Mohammadi, Normal cross—sectional anatomy of the bovine digit: comparison of computed tomography and limb anatomy, *Journal of Veterinary Medicine Series C: Anatomia Histologia Embryologia*, **37**, no. 3, 188–191, (2008).

[26] O. Schaller, *Illustrated Veterinary Anatomical Nomenclature*, Enke Verlag, Stuttgart, Germany, 1992.

[27] J. K. Shearer and S. R. Van Amstel, Functional and corrective claw trimming, *The Veterinary Clinics of North America. Food Animal Practice*, **17**, no. 1, 53–72, (2001).

[28] G. C. Skerrit and J. McLelland, *An Introduction to the Functional Anatomy of the Limbs of the Domestic Animals*, John Wright & Sons, Bristol, UK, 1984.

[29] M. Soler, J. Murciano, R. Latorre, E. Belda, M. J. Rodríguez, and A. Agut, Ultrasonographic, computed tomographic and magnetic resonance imaging anatomy of the normal canine stifle joint, *The Veterinary Journal*, **174**, no. 2, 351–361, (2007).

[30] D. D. Stark and W. G. Bradley, *Magnetic Resonance Imaging*, **2**, Mosby, St Louis, Mo, USA, 3rd edition, 1999.

[31] G. O. Van der Straaten, S. N. Collins, A. B. Rijkenhuizen, and R. C. Murray, *Magnetic resonance imaging of the equine stifle: normal anatomy [M.S. thesis]*, Utrecht University, Utrecht, The Netherlands, 2009.

[32] A. D. Weaver, Lameness above the foot, in *Chapter 32 Bovine Medicine (Diseases and Husbandry of Cattle)*, A. H. Andrews, R.W. Blowey, H. Boyd, and R. G. Eddy, Eds., Blackwell Science Ltd a Blackwell Publishing, 2nd edition, 2004.